Bioorganic & Medicinal Chemistry Letters 22 (2012) 7371–7375

Contents lists available at SciVerse ScienceDirect

Bioorganic & Medicinal Chemistry Letters

journal homepage: www.elsevier.com/locate/bmcl

Discovery of selective biaryl ethers as PDE10A inhibitors: Improvement in potency and mitigation of Pgp-mediated efflux

Robert M. Rzasa [a,*], Essa Hu [a], Shannon Rumfelt [a], Ning Chen [a], Kristin L. Andrews [c], Samer Chmait [c], James R. Falsey [a], Wenge Zhong [a], Adrie D. Jones [d], Amy Porter [b], Steven W. Louie [e], Xiaoning Zhao [d], James J. S. Treanor [b], Jennifer R. Allen [a]

[a] Department of Medicinal Chemistry, Amgen Inc., One Amgen Center Drive, Thousand Oaks, CA 91320-1799, USA
[b] Department of Neuroscience, Amgen Inc., One Amgen Center Drive, Thousand Oaks, CA 91320-1799, USA
[c] Department of Molecular Structure and Characterization, Amgen Inc., One Amgen Center Drive, Thousand Oaks, CA 91320-1799, USA
[d] Department of Molecular Structure and Characterization, Amgen Inc., 1120 Veterans Boulevard, So San Francisco, CA 94080-1985, USA
[e] Department of Pharmacokenetics and Drug Metabolism, Amgen Inc., One Amgen Center Drive, Thousand Oaks, CA 91320-1799, USA

ARTICLE INFO

Article history:
Received 21 August 2012
Revised 5 October 2012
Accepted 15 October 2012
Available online 22 October 2012

Keywords:
Phosphodiesterase
PDE10A
Inhibitors
Pgp-mediated efflux
Schizophrenia

ABSTRACT

We report the discovery of a novel series of biaryl ethers as potent and selective PDE10A inhibitors. Structure–activity studies improved the potency and decreased Pgp-mediated efflux found in the initial compound **4**. X-ray crystallographic studies revealed two novel binding modes to the catalytic site of the PDE10A enzyme.

Cyclic phosphodiesterases (PDE) are enzymes that regulate cellular signaling by hydrolyzing the 3′-5′phosphodiester bond of secondary messengers cyclic adenosine mono phosphate (cAMP) and cyclic guanosine mono phosphate (cGMP).[1] Deregulation of PDEs has been implicated in various diseases such as cardiovascular disease, neurodegenerative disorders, inflammation and cancer.[1,2] PDE enzymes constitute a diverse, 11-membered family of isozymes that differ in their substrate specificity and tissue distribution.[3] Specifically, PDE10A is a dual specificity phosphodiesterase that is predominantly expressed in the medium spiny neurons of the striatum.[4,5] Inhibition of PDE10A effectively increases the striatal levels of cAMP/cGMP resulting in modulation of neuronal activity.[6] Evidence suggests inhibition of PDE10A can be a novel mechanism for the treatment for neurological disorders such as schizophrenia.[7,8]

Although current medications have demonstrated effectiveness in treating positive symptoms of schizophrenia (delusions, hallucinations, disorganized behavior and speech) they are ineffective in treating negative symptoms (apathy, anhedonia, social withdrawal) and cognition disorders. In addition, diabetes, weight gain, QT prolongation and extrapyramidal syndrome are common side effects associated with current treatments.[9] To address the negative symptoms and minimize side effects associated with antipsychotic medications, the development of PDE10A inhibitors as antipsychotic drugs has attracted extensive research efforts over the past several years.[10] In particular, the alkaloid papaverine **1** (Fig. 1) has demonstrated in vivo efficacy in clinically relevant animal models producing dose dependent inhibition in the conditioned avoidance response (CAR) and phencyclidine (PCP)-induced hyperactivity models in rodents.[6] Pfizer is currently evaluating the PDE10A inhibitor MP-10 (**2**) in clinical trials.[11]

Recently, we disclosed our structure-activity relationships investigation into a novel class of cinnolines as PDE10A inhibitors exemplified by compound **3**.[10k] As part of our on-going efforts to develop a PDE10A inhibitor for the treatment of schizophrenia, we identified compound **4** as a modestly potent and selective PDE10A inhibitor (Fig. 2). Although compound **4** exhibited good cellular permeability it also displayed high P-glycoprotein (Pgp)-mediated efflux. It is well known in the literature that molecular descriptors related to hydrogen bonding (hydrogen bond acceptor count, hydrogen bond donor count, and topological polar surface area) can have an instrumental effect in reducing passive permeability and increasing efflux.[12] Recognizing that Pgp susceptibility is known to have a dramatic influence on compounds targeting the CNS,[13] we included permeability and efflux assays into our

* Corresponding author.
E-mail address: rrzasa@amgen.com (R.M. Rzasa).

0960-894X/$ - see front matter © 2012 Elsevier Ltd. All rights reserved.
http://dx.doi.org/10.1016/j.bmcl.2012.10.078

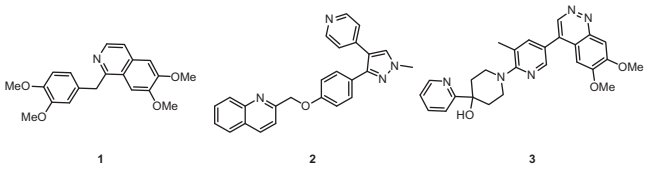

Figure 1. PDE10A inhibitors.

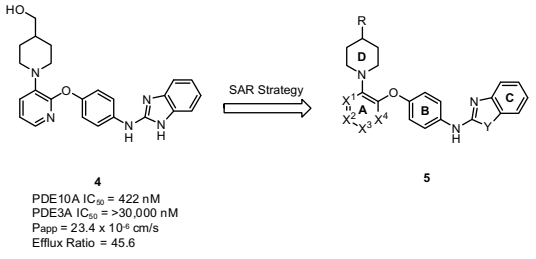

Figure 2. PDE10A SAR strategy.

screening paradigm. Thus, the goal of this investigation was not only to improve PDE10A potency but to decrease Pgp susceptibility of our newly identified lead molecule **4**. In this report we describe our SAR strategy into biaryl ethers **5** as potential PDE10A inhibitors for the treatment of schizophrenia.

The derivatives prepared in this study were evaluated for their ability to inhibit purified recombinant human PDE10A and screened for PDE3A selectivity.[14,15] Compounds were evaluated for in vitro metabolic stability using a human liver microsomal assay (HLM). Passive permeability was determined using parental LLC-PK cells whereas Pgp-mediated efflux was determined using LLC-PK cells transfected with human MDR1.[16]

The first derivatives examined in this study were compounds with various A-ring modifications (Table 1). The preliminary data for compound **4** are included for comparison. Gratifyingly, phenyl analog **6** was 448-fold more potent against PDE10A versus compound **4**. Pyridine isomers **7** and **8** resulted in >4000-fold improvement in potency at the expense of decreased microsomal stability. Interestingly, diazines were also potent PDE10A inhibitors but position of the nitrogen atoms in the A-ring was critical. In comparison to compound **4**, pyrimidine **9** displayed a >800-fold improvement in potency whereas the pyridazine analog **10** resulted in a 14-fold loss in potency. Pyrazine **11** showed the most significant improvement in potency (>4500-fold, **11** vs **4**). Diazines were also more metabolically stable than their pyridine and phenyl counterparts (**9**–**11** vs **6–8**). Unfortunately, while our initial efforts to improve potency and maintain PDE3A selectivity were successful in producing highly permeable compounds, high efflux remained an issue.

Encouraged by these initial results, we proceeded with our investigation by modifying the C-ring of compound **11** to mitigate Pgp-mediated efflux (Table 2). We hypothesized the high efflux resulted from the presence of the amino-benzimidazole moiety.[17] Our strategy to lower efflux was to remove the hydrogen bond donor present in the benzimidazole. In general, replacement of the NH of the benzimidazole maintained cellular permeability and decreased efflux. We were pleased when the N-methyl benzimidazole **12** displayed equal potency and lower efflux (>10-fold) in comparison to compound **11**. Although benzoxazole **13** exhibited an fivefold loss in potency, the compound showed a further reduction in efflux (**13** vs **11**). Ultimately, the most significant improvement in lowering efflux was achieved by replacing the benzimidazole C-ring with a benzothiazole (**14** vs **11**).

Further SAR investigations focusing on modifications to the D-ring of compound **14** are shown in Table 3. In general, the addition of alkyl groups in the 4-position of the piperidine D-ring decreased potency. For instance, the methoxy analog **15** led to a >90-fold decrease in potency in addition to decreased microsomal stability. The secondary alcohol **16** led to a 12-fold loss in potency while tertiary alcohols **17** and **18** resulted in >21-fold and >690-fold loss in enzyme inhibition, respectively. Although acid **19** showed a modest 14-fold loss in activity and exhibited good passive permeability, compound **19** displayed increased Pgp-mediated efflux, presumeably due to its high polar surface area (PSA 100 Å^2).

Determination of the cocrystal structure of compound **7** bound to human PDE10A provided insights into the potency and selectivity of this class of molecules (Fig. 3). Several important ligand-protein interactions were observed. First, the hydroxyl moiety of the piperidine displaces a water molecule in the lipophilic Q1 pocket of the catalytic site forming an H-bond with the backbone carbonyl oxygen of Thr675 and a water mediated H-bond with the conserved Gln716. This deep penetration into the catalytic site may explain the high potency for compound **7**. Second, the benzimidazole group occupies the Q2 selectivity pocket adjacent to the sidechain of Met703 and the nitrogen on the benzimidazole forms an H-bond with Tyr683. The occurrence of the small residue Gly715, present only in PDE10A, allows these compounds access to this pocket which may explain the high selectivity over other PDEs.[18] Lastly, the biaryl ether forms hydrophobic interactions with the hydrophobic clamp as defined by residues Phe719, Phe686 and Ile682. The phenyl ring forms an edge-to-face π-interaction with Phe719 whereas the pyridyl group forms hydrophobic interactions with Phe686 and Ile682.

In contrast, the X-ray crystallographic data of compound **16** in PDE10A revealed an alternative binding orientation this series of compounds may adopt within the active site (Fig. 4). The presence of the hydroxyethyl group on the piperidine D-ring of compound **16** is sufficiently large to orient the ligand into a different binding mode within the catalytic site of enzyme. The ligand does not access the Q1 pocket but positions the 4-hydroxyethyl-piperidine toward the water coordinated metal site. The N-1 nitrogen of the pyrazine forms a direct hydrogen bond with Gln716. Similar to the benzimidazole of compound **7**, the benzothiazole occupies the Q2 selectivity pocket with the N-3 nitrogen forming a hydrogen bond to Tyr683. The phenyl ring is positioned within the hydrophobic clamp forming an edge-face interaction with Phe719 and a face-edge interaction with Phe686.

The compounds required for this investigation were prepared by a variety of routes using S_NAr or metal-mediated coupling strategies. Various routes were utilized in the preparation of the desired analogs and the particular route employed was dictated by the availability of appropriate starting materials. Pyridine **4**, pyridazine **10**, and pyrazines **11-13** were prepared in three steps as outlined in Scheme 1. Nucleophilic displacement of the appropiate chloro heterocycle **20**–**22**[19] with 4-aminophenol and cesium carbonate at 90–100 °C selectively gave compound **23**. Introduction of the 4-(hydroxymethyl)piperidine group under palladium catalyzed or nucleophilic displacement conditions smoothly provided aniline **24**. Final displacement using 2-chlorobenzimidazole under microwave heating gave compounds **4**, **10** and **11**. Likewise, treatment of compound **24** with either 1-methyl-2-chlorobenzimidazole or 2-chlorobenzoxazole gave compounds **12** and **13**, respectively.

Alternatively, pyridine analogs **7** and **8** were prepared in three steps from 2-chlorobenzimidazole as shown in Scheme 2. Reaction between 4-aminophenol and 2-chlorobenzimidazole **25** in the absence of base gave selectively the nitrogen linked phenol **26**. Treatment of either 3-fluoro-2-nitropyridine or 3-bromo-4-chloropyridine with compound **26** gave compounds **27** and **28**, respectively. Final displacement of the nitro group of **27** or copper

Table 1
PDE10A inhibitory activity of A-ring modified analogs

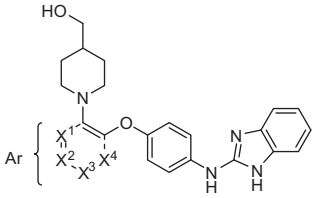

Compd.	Ar	PDE10A[a]	PDE3A[a]	HLM[b]	P_{app}[c]	ER[d]
4		422	>30,000	52	23.4	45.6
6		0.941	>30,000	315	13.0	10.6
7		0.097	>30,000	277	75.2	49.5
8		0.075	>30,000	142	15.8	42.1
9		0.521	>30,000	76	26.2	>92
10		6210	>30,000	22	44.0	79.3
11		0.092	>30,000	41	41.6	76.7

[a] IC_{50} values (nM) are the means of at least two independent experiments.
[b] mL/(min mg).
[c] Apparent permeability rates (10^{-6} cm/s) through porcine proximal tubule cells (LLC-PK1 cell line).
[d] Efflux ratio (ER).

Table 2
PDE10A inhibitory activity of C-ring modified analogs

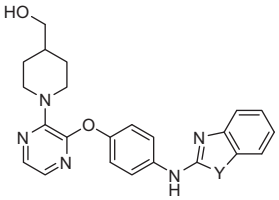

Compd.	Y	PDE10A[a]	PDE3A[a]	HLM[b]	P_{app}[c]	ER[d]
11	NH	0.092	>30,000	41	41.6	76.7
12	NMe	0.056	>30,000	15	39.4	6.0
13	O	0.513	>30,000	54	23.7	3.4
14	S	0.199	>30,000	62	8.0	1.1

[a] IC_{50} values (nM) are the means of at least two independent experiments.
[b] mL/(min mg).
[c] Apparent permeability rates (10^{-6} cm/s) through porcine proximal tubule cells (LLC-PK1 cell line).
[d] Efflux ratio (ER).

mediated coupling of **28** with 4-(hydroxymethyl)piperidine yielded compounds **7** and **8**, respectively.

Compounds **6** and **9**, wherein the A-ring was either benzene or pyrimidine rings, were prepared as shown in Scheme 3. Intermediates **31** and **32** were prepared as follows: palladium catalyzed coupling of ethyl isonipecolate to 2-bromoanisole **29** followed by

Table 3
PDE10A inhibitory activity of D-ring modified analogs

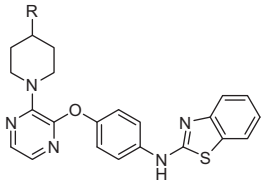

Compd.	R	PDE10A[a]	PDE3A[a]	HLM[b]	P_{app}[c]	ER[d]
14		0.199	>30,000	62	8.0	1.1
15		19.3	>30,000	166	10.5	1.3
16		2.4	>30,000	98	2.3	1.1
17		4.2	>30,000	72	12.6	2.9
18	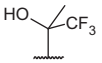	138	>30,000	18	3.7	1.8
19		2.82	>30,000	<14	35.3	12.8

[a] IC_{50} values (nM) are the means of at least two independent experiments.
[b] mL/(min mg).
[c] Apparent permeability rates (10^{-6} cm/s) through porcine proximal tubule cells (LLC-PK1 cell line).
[d] Efflux ratio (ER).

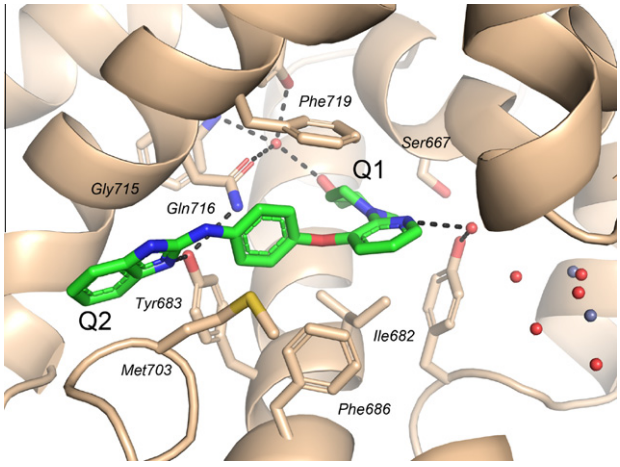

Figure 3. 2.0 Å Cocrystal of **7** (green) and human PDE10A (PDB ID code 4HEU). Key hydrogen bond interactions are represented as black dash lines, red spheres indicate water molecules (some water molecules have been omitted for clarity) and purple spheres indicate zinc atoms.

lithium aluminum hydride reduction and demethylation with sodium iodide gave phenol **31**. Attempts to couple 4-(hydroxymethyl)piperidine to either 2-bromoanisole or 2-iodoanisole directly failed to give the desired coupling product. In the case of intermediate **32** commercially available 4,6-dichloro-5-methoxypyrimidine **30** was treated with 4-(hydroxymethyl)piperidine. Removal of the second chlorine atom by hydrogenation followed by demethylation provided pyrimidine **32**. Intermediates **31** and **32** were treated with 1-fluoro-4-nitrobenzene followed by reduction of the nitro moiety giving intermediates **33** and **34** which, upon reaction with 2-chlorobenzimidazole under microwave conditions, provided compounds **6** and **9**, respectively.

Pyrazines **14**–**19**, with modifications to the D-ring, were synthesized in three steps beginning with 2-chlorobenzothiazole

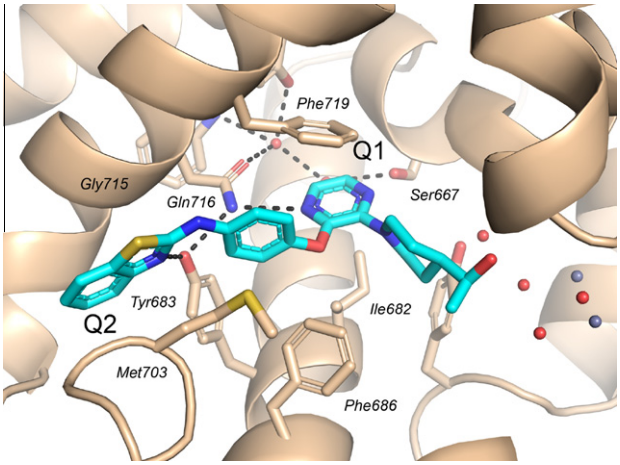

Figure 4. 2.0 Å Cocrystal of **16** (cyan) with human PDE10A (PDB ID code 4HF4). Key hydrogen bond interactions are represented as black dash lines, red spheres indicate water molecules (some water molecules have been omitted for clarity) and purple spheres indicate zinc atoms.

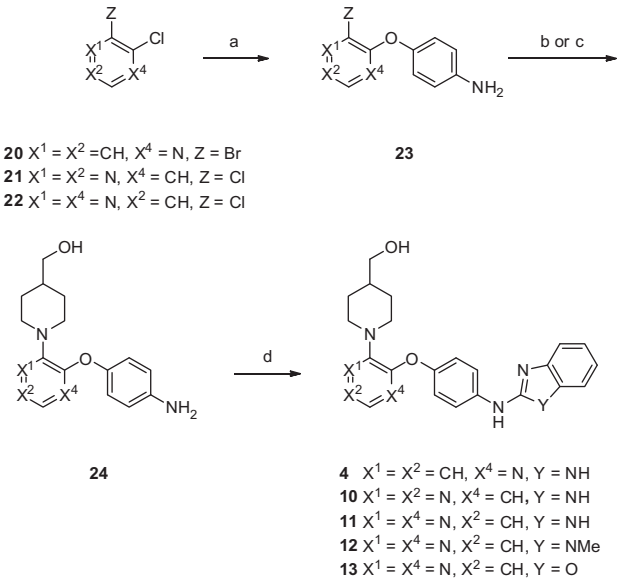

Scheme 1. Reagents and conditions: (a) 4-aminophenol, Cs_2CO_3, DMSO, 90–100 °C, 63–91%; (b) 4-(hydroxymethyl)piperidine, $Pd_2(dba)_3$, Xantphos, NaO*t*Bu, toluene, 100 °C; (c) 4-(hydroxymethyl)piperidine, *i*PrOH, μW, 160 °C, 30 min; (d) 2-chlorobenzimidazole, 2-chloro-1-methylbenzimidazole, or 2-chloro-benzoxazole, *i*PrOH, μW, 160 °C, 30 min, 5–35% (2 steps).

(Scheme 4). Treatment of 2-chlorobenzothiazole **35** with 4-aminophenol gave compound **36** which was reacted with 2,3-dichloropyrazine under basic conditions to yield compound **37**. Subsequent chloride displacement with a variety of substituted piperidines provided compounds **14–19**.

In summary, a series of potent and selective biaryl ether PDE10A inhibitors was discovered. Structure-activity relationship studies resulted in >10,000-fold improvement in potency while maintaining PDE3A selectivity. The issue of high Pgp-mediated efflux was addressed by removing a hydrogen bond donor from the benzimidazole C-ring. X-ray crystallographic data suggested that compounds of this series may adopt one of two different binding modes depending on the substitutent present in the 4-position of the D-ring. The bicyclic C-ring in this series of inhibitors occupies the unique Q2 pocket resulting in high selectivity among other PDEs.

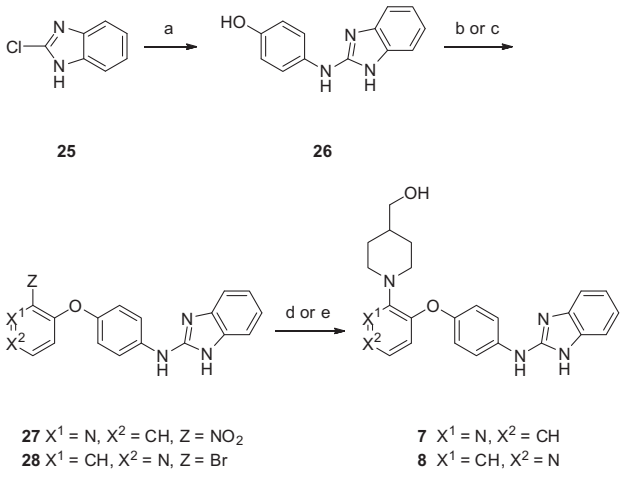

Scheme 2. Reagents and conditions: (a) 4-aminophenol, HCl, EtOH, reflux, 72%; (b) 3-fluoro-2-nitropyridine, K_2CO_3, DMSO, 60 °C, 42%; (c) 3-bromo-4-chloropyridine, Cs_2CO_3, DMSO, 90 °C; (d) 4-(hydroxymethyl)piperidine, K_2CO_3, DMSO, 110 °C, 35%; (e) 4-(hydroxymethyl)piperidine, Cu, CsOAc, DMSO, 150 °C (1%, 2 steps).

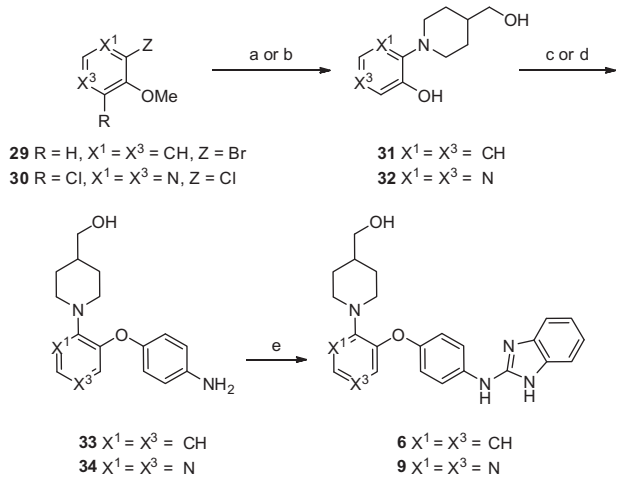

Scheme 3. Reagents and conditions: (a) (i) ethyl isonipecolate, Pd_2dba_3, BINAP, NaO*t*Bu, toluene, 105 °C, 64%; (ii) LAH, THF, 0 °C; (iii) NaI, pyridine, 200 °C, μW, 3 h, (50%, 2 steps), (b) (iv) 4-(hydroxymethyl)piperidine, K_2CO_3, DMSO, rt, 86%; (v) Pd/C, H-cube, 74%; (vi) LiI, pyridine, 200 °C, μW, 3 h, (c) (vii) 1-fluoro-4-nitrobenzene, Cs_2CO_3, DMSO, rt, 57%; (viii) Fe dust, AcOH, aq EtOH, 65 °C, (97%), (d) (ix) 1-fluoro-4-nitrobenzene, Cs_2CO_3, DMSO, 80 °C, (62% 2 steps); (x) Pd/C, MeOH, H-cube, 48–84%, (e) 2-chlorobenzimidazole, *i*PrOH, 120–160 °C, μW, 17–42%.

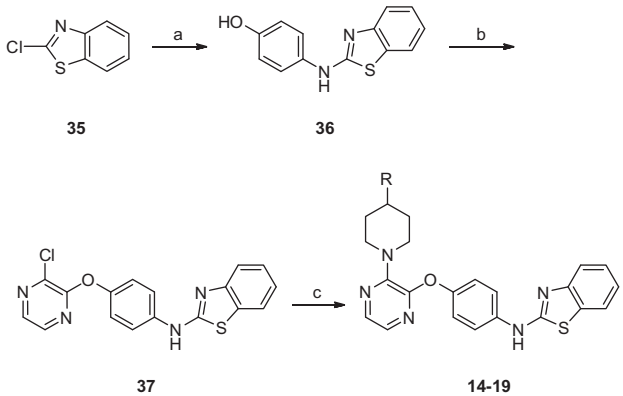

Scheme 4. Reagents and conditions: (a) 4-aminophenol, NMP, 160 °C, 71%; (b) 2,3-dichloropyrazine, Cs_2CO_3, DMSO, 80 °C, 66%; (c) 4-substituted piperidine, DMSO, 60 °C, 34–73%.

Acknowledgments

The authors would like to thank Dr. Andreas Reichelt, Dr. Lewis Pennington and Dr. Markian Stec for their insightful discussions and suggestions. The authors also thank the Advanced Light Source staff at beamline 5.0.2 for their support. The Advanced Light Source is supported by the Director, Office of Science, Office of Basic Energy Sciences, Materials Sciences Division, of the U.S. Department of Energy under Contract DE-AC03-76SF00098 at Lawrence Berkeley National Laboratory.

References and notes

1. Bender, A. T.; Beavo, J. A. *Pharmacol. Rev.* **2006**, *58*, 488.
2. Keravis, T.; Lugnier, C. *Br. J. Pharmacol.* **2012**, *165*, 1288.
3. Lakics, V.; Karran, E. H.; Boess, F. G. *Neuropharmacology* **2010**, *59*, 367.
4. (a) Soderling, S. H.; Bayuga, S. J.; Beavo, J. A. *Proc. Natl. Acad. Sci. U.S.A.* **1999**, *96*, 7071; (b) Loughney, K.; Snyder, P. B.; Uher, L.; Rosman, G. J.; Ferguson, K.; Florio, V. A. *Gene* **1999**, *234*, 109; (c) Fujishige, K.; Kotera, J.; Michibata, H.; Yuasa, K.; Takebayashi, S.; Okumura, K.; Omori, K. *J. Biol. Chem.* **1999**, *274*, 18438.
5. Xie, Z.; Adamowicz, W. O.; Eldred, W. D.; Jakowski, A. B.; Kleiman, R. J.; Morton, D. G.; Stephenson, D. T.; Strick, C. A.; Williams, R. D.; Menniti, F. S. *Neuroscience* **2006**, *139*, 597.
6. (a) Siuciak, J. A.; McCarthy, S. A.; Chapin, D. S.; Fujiwara, R. A.; James, L. C.; Williams, R. D.; Stock, J. L.; McNeish, J. D.; Strick, C. A.; Menniti, F. S.; Schmidt, C. J. *Neuropharmacology* **2006**, *51*, 374; (b) Siuciak, J. A.; Chapin, D. S.; Harms, J. F.; Lebel, L. A.; McCarthy, S. A.; Chambers, L.; Shrikhande, A.; Wong, S.; Menniti, F. S.; Schmidt, C. J. *Neuropharmacology* **2006**, *51*, 386.
7. (a) Suiciak, J. A. *CNS Drugs* **2008**, *22*, 983; (b) Menniti, F. S.; Chappie, T. A.; Humphrey, J. M.; Schmidt, C. J. *Curr Opin. Investig. Drugs* **2007**, *8*, 54.
8. For implications to Huntington's disease see: (a) Giampa, C.; Patassini, S.; Borreca, A.; Laurenti, D.; Marullo, F.; Bernardi, G.; Menniti, F.; Fusco, F. R. *Neurobiol. Dis.* **2009**, *34*, 450; (b) Kleiman, R. J.; Kimmel, L. H.; Bove, S. E.; Lanz, T. A.; Harms, J. F.; Romegialli, A.; Miller, K. S.; Willis, A.; des Etages, S.; Kuhn, M.; Schmidt, C. J. *J. Pharmacol. Exp. Ther.* **2011**, *336*, 64.
9. (a) Newcomer, J. W. *CNS Drugs* **2005**, *19*, 1; (b) Taylor, D. M. *Acta Psychiatr. Scand.* **2003**, *107*, 85; (c) Casey, D. E. *Am. J. Med.* **2005**, *118*, 15S; (d) Dayalu, P.; Chou, K. L. *Expert Opin. Pharmacother.* **2008**, *9*, 1451.
10. (a) Chappie, T. A.; Humphrey, J. M.; Allen, M. P.; Estep, K. G.; Fox, C. B.; Lebel, L. A.; Liras, S.; Marr, E. S.; Menniti, F. S.; Pandit, J.; Schmidt, C. J.; Tu, M.; Williams, R. D.; Yang, F. V. *J. Med. Chem.* **2007**, *50*, 182; (b) Cantin, L.-D.; Magnuson, S.; Gunn, D.; Barucci, N.; Breuhaus, M.; Bullock, W. H.; Burke, J.; Claus, T. H.; Daly, M.; DeCarr, L.; Gre-Willse, A.; Hoover-Litty, H.; Kumarasinghe, E. S.; Li, Y.; Liang, S. X.; Livingston, J. N.; Lowinger, T.; MacDougall, M.; Ogutu, H. O.; Olague, A.; Otto-Morgan, R.; Schoenleber, R. W.; Tersteegen, A.; Wickens, P.; Zhang, Z.; Zhu, J.; Zhu, L.; Sweet, L. *Bioorg. Med. Chem. Lett.* **2007**, *17*, 2869; (c) Höfgen, N.; Stange, H.; Schindler, R.; Lankau, H.-J.; Grunwald, C.; Langen, B.; Egerland, U.; Tremmel, P.; Pangalos, M. N.; Marquis, K. L.; Hage, T.; Harrison, B. L.; Malamas, M. S.; Brandon, N. J.; Kronbach, T. *J. Med. Chem.* **2010**, *53*, 4399; (d) Helal, C. J.; Kang, Z.; Hou, X.; Pandit, J.; Chappie, T. A.; Humphrey, J. M.; Marr, E. S.; Fennell, K. F.; Chenard, L. K.; Fox, C.; Schmidt, C. J.; Williams, R. D.; Chapin, D. S.; Siuciak, J.; Lebel, L.; Menniti, F.; Cianfrongna, J.; Fronseca, K. R.; Nelson, F. R.; O'Connor, R.; MacDougall, M.; McDowell, L.; Liras, S. *J. Med. Chem.* **2011**, *54*, 4536; (e) Kehler, J.; Ritzen, A.; Langgård, M.; Petersen, S. L.; Farah, M. M.; Bundgaard, C.; Chirstoffersen, C. T.; Nielsen, J.; Kilburn, J. P. *Bioorg. Med. Chem. Lett.* **2011**, *21*, 3738; (f) Gage, J. L.; Onrust, R.; Johnston, D.; Osnowski, A.; MacDonald, W.; Mitchell, L.; Ürögdi, L.; Rohde, A.; Harbol, K.; Gragerov, S.; Dormán, G.; Wheeler, T.; Florio, V.; Cutshall, N. S. *Bioorg. Med. Chem. Lett.* **2011**, *21*, 4155; (g) Yang, S.-W.; Smotryski, J.; McElroy, W. T.; Tan, Z.; Ho, G.; Tulshian, D.; Greenlee, W. J.; Guzzi, M.; Zhang, X.; Mullins, D.; Xiao, L.; Hruza, A.; Chan, T.-M.; Rindgen, D.; Bleickardt, C.; Hodgson, R. *Bioorg. Med. Chem. Lett.* **2012**, *22*, 235; (h) Ho, G. D.; Yang, S.-W.; Smotryski, J.; Bercovici, A.; Nechuta, T.; Smith, E. M.; McElroy, W.; Tan, Z.; Tulshian, D.; McKittrick, B.; Greenlee, W. J.; Hruza, A.; Xiao, L.; Rindgen, D.; Mullins, D.; Guzzi, M.; Zhang, X.; Bleickardt, C.; Hodgson, R. *Bioorg. Med. Chem. Lett.* **2012**, *22*, 1019; (i) McElroy, W. T.; Tan, Z.; Basu, K.; Yang, S.-W.; Smotryski, J.; Ho, G. D.; Tulsian, D.; Greenlee, W. J.; Mullins, D.; Guzzi, M.; Zhang, X.; Bleickardt, C.; Hodgson, R. *Bioorg. Med. Chem. Lett.* **2012**, *22*, 1335; (j) Bauer, U.; Giordanetto, F.; Bauer, M.; O'Mahony, G.; Johansson, K. E.; Knecht, W.; Hartleib-Geschwindner, J.; Carlsson, E. T.; Enroth, C. *Bioorg. Med. Chem. Lett.* **1944**, *2012*, 22; (k) Hu, E.; Kunz, R. K.; Rumfelt, S.; Chen, N.; Bürli, R.; Li, C.; Andrews, K. L.; Zhang, J.; Chmait, S.; Kogan, J.; Lindstrom, M.; Hitchcock, S. A.; Treanor, J. *Bioorg. Med. Chem. Lett.* **2012**, *22*, 2262; (l) Ho, G. D.; Seganish, W. M.; Bercovici, A.; Tulshian, D.; Greenlee, W. J.; Van Rijn, R.; Hruza, A.; Xiao, L.; Rindgen, D.; Mullins, D.; Guzzi, M.; Zhang, X.; Bleickardt, C.; Hodgson, R. *Bioorg. Med. Chem. Lett.* **2012**, *22*, 2585.
11. Verhoest, P. R.; Chapin, D. S.; Corman, M.; Fonseca, K.; Harms, J. F.; Hou, X.; Mar, E. S.; Menniti, F. S.; Nelson, F.; O'Connor, R.; Pandit, J.; Proulx-LaFrance, C.; Schmidt, A. W.; Schmidt, C. J.; Siuciak, J. A.; Liras, S. *J. Med. Chem.* **2009**, *52*, 5188.
12. (a) Raub, T. J. *Mol. Pharm.* **2006**, *3*, 3; (b) Hitchcock, S. A. *J. Med. Chem.* **2012**, *55*, 4877.
13. (a) Balimane, P. V.; Han, Y.-H.; Chong, S. *The AAPS J.* **2006**, *8*, E1; (b) Feng, B.; Mills, J. B.; Davidson, R. E.; Mireles, R. J.; Janiszewski, J. S.; Troutman, M. D.; de Morais, S. M. *Drug Metab. Dispos.* **2008**, *36*, 268; (c) He, H.; Lyons, K. A.; Shen, X.; Yao, Z.; Bleasby, K.; Chan, G.; Hafey, M.; Li, X.; Xu, S.; Salituro, G. M.; Cohen, L. H.; Tang, W. *Xenobiotica* **2009**, *39*, 687.
14. Inhibition of PDE3 has been associated with undesirable cardiovascular effects. See: (a) Sugiyama, A.; Satoh, Y.; Hashimoto, K. *J. Cardiovasc. Pharmacol.* **2001**, *38*, 268; (b) Van de Water, A.; D'Aubioul, J.; Van Gervan, W.; De Chaffoy de Courcelles, D.; Freyne, E.; Xhonneux, R.; Reneman, R. S.; Janssen, P. A. J. *Arch. Int. Pharmacodyn. Ther.* **1992**, *316*, 60.
15. The purified human PDE3A and PDE10A2 enzymes were obtained from BPS Bioscience (San Deigo, CA). IMAPTM TR-FRET progressive binding system, FAM-cAMP substrate were from molecular devices (Sunnyvale, CA). The PDE IMAP assay was conducted in a 384-well black Greiner polypropylene plate (Sigma, St. Louis, MO). PDE inhibitors were serial diluted in 100% DMSO and dispensed into assay plate at 200 nL per well using Echo® Liquid Handling System from LABCYTE. 10 μL of PDE enzyme in IMAP reaction buffer (10 mM Tris–HCL, pH 7.2, 10 mM $MgCl_2$, 0.05% NaN_3, and 0.01% Tween-20) was added into the assay wells. The PDE enzyme concentration used was based on each lot of enzyme activity, to ensure enzyme reaction falls in a linear range under assay condition. 0.2 nM of PDE3 or 8 pM PDE10 were used in the assay system. Enzyme was pre-incubated with inhibitors for 60 min at room temperature before addition of 10 μL of substrate addition, which results in 100 nM of FAM-cAMP in the reaction. Enzyme reaction was allowed to proceed at room temperature for 90 min, and the reaction is stopped by 55 μl addition of binding reagent according to manufacturer's recommendation. The mixture is further incubated at room temperature for additional 4 hours, and signal was read on an Envision multimode reader (PerkinElmer). Fluorescence signals were measured at 520 and 485 nm. The signal ratio at 520/485 nm corresponded to the generation of reaction product of AMP, and it was used in all data analysis. Values from DMSO-treated wells were normalized to POC = 100, and no-enzyme wells were normalized to POC = 0. IC_{50} values were determined by using the Genedata Screener V9.0.1.The curve fitting algorithm used for dose response data analysis in Genedata Screener is a custom implementation of a robust curve-fitting algorithm called ROUT (Robust regression with outlier detection) and uses a four-parameter logistical (4PL) Hill model.
16. For a detailed description of assays performed in this study see: Hu, E.; Ma, J.; Biorn, C.; Lester-Zeiner, D.; Cho, R.; Rumfelt, S.; Kunz, R. K.; Nixey, T.; Michelson, K.; Miller, S.; Shi, J.; Wong, J.; Hill Della Puppa, G.; Able, J.; Taljeda, S.; Hwang, D.-R.; Hitchcock, S. A.; Porter, A.; Immke, D.; Allen, J. R.; Treanor, J.; Chen, H. *J. Med. Chem.* **2012**, *55*, 4776.
17. For a similar strategy of masking the NH of a benzimidazole to reduce Pgp susceptibility see: Bergman, J. M.; Roecker, A. J.; Mercer, S. P.; Bednar, R. A.; Reiss, D. R.; Ransom, R. W.; Harrell, C. M.; Pettibone, D. J.; Lemaire, W.; Murphy, K. L.; Li, C.; Prueksaritanont, T.; Winrow, C. J.; Renger, J. J.; Koblan, K. S.; Hartman, G. D.; Coleman, P. J. *Bioorg. Med. Chem. Lett.* **2008**, *18*, 1425.
18. All compounds reported in this investigation showed selectivity against PDE2A, PDE3A and PDE4D at IC_{50} >10 μM with the exception of compound **13** (PDE4D IC_{50} 7.4 μM).
19. For the preparation of 3,4-dichloropyridazine 21 see: Yanai, M.; Kinoshita, T. *Yakugaku Zasshi* **1965**, *85*, 344.